Available online at www.sciencedirect.com
SCIENCE DIRECT
Cement and Concrete Research 36 (2006) 305 – 319
Cement and Concrete Research

Characterisation of the surface thermodynamic properties of cement components by inverse gas chromatography at infinite dilution

Christian Perruchot[a], Mohamed M. Chehimi[a], Marie-Josèphe Vaulay[a], Karim Benzarti[b,*]

[a]*Interfaces, Traitements, Organisation et Dynamique des Systèmes (ITODYS), Université Paris 7- Denis. Diderot, 1 Rue Guy de la Brosse, 75005 Paris, France*
[b]*Laboratoire Central des Ponts et Chaussées (LCPC), 58 Boulevard Lefèvre, 75732 Paris Cedex 15, France*

Received 13 November 2003; accepted 21 February 2005

Abstract

The surface thermodynamic properties of three main inorganic compounds formed during hydration of Portland cement: calcium hydroxide ($Ca(OH)_2$), ettringite ($3CaO{\cdot}Al_2O_3{\cdot}3CaSO_4{\cdot}32H_2O$) and calcium-silicate-hydrates (C-S-H), respectively, and one mineral filler: calcium carbonate ($CaCO_3$), have been characterised by inverse gas chromatography at infinite dilution (IGC-ID) at 35 °C. The thermodynamic properties have been investigated using a wide range of non-polar (*n*-alkane series), Lewis acidic (CH_2Cl_2 and $CHCl_3$), Lewis basic (diethyl ether) and aromatic (benzene) and *n*-alkene series molecular probes, respectively. The tested samples are fairly high surface energy materials as judged by the high dispersive contribution to the total surface energy (the dispersive components γ_s^d range from 45.6 up to 236.2 mJ m^{-2} at 35 °C) and exhibit amphoteric properties, with a predominant acidic character. In the case of hydrated components (i.e. ettringite and C-S-H), the surface thermodynamic properties have been determined at various temperatures (from 35 up to 120 °C) in order to examine the influence of the water content. The changes of both dispersive and specific components clearly demonstrate that the material surface properties are activated with temperature. The changes in the acid–base properties are correlated with the extent of the overall water loss induced by the thermal treatment as demonstrated by thermogravimetric analysis (TGA). The elemental surface composition of these compounds has been determined by X-ray photoelectron spectroscopy (XPS).

Keywords: Cement paste components; Inverse gas chromatography; Surface energy; Dispersive and acid–base interactions; TGA; XPS

1. Introduction

In the fields of civil engineering and construction, functionalised polymeric materials bearing amino- or epoxy-reactive end groups received increasing interest for the repair of damaged buildings and bridges. Two common applications are the filling of cracks in existing concrete structures and the reinforcement by adhesively bonded composite materials. These processes can also be used to prevent crumble or metal corrosion induced by water diffusion into porous walls. Moreover, the conception of new architectural structures could be achieved in the near future by assembling concrete elements to each other via polymeric resins.

Long term durability of the adhesive joint is thus of fundamental and applied importance in order to prevent failure of the resulting assemblies during the whole service life of the structure [1].

Adhesion phenomena are closely related to physical and chemical molecular interactions between the concrete surface and the polymeric resins. Therefore, it is necessary to improve our fundamental knowledge regarding the surface physico–chemical properties of cementitious materials in order to predict interactions likely to occur at the concrete-polymer interface.

The role of dispersive and acid–base interactions is of great importance in the field of adhesion and for adsorption of polymeric materials at the surface of planar or finely divided inorganic materials [2]. In his pioneering studies, Fowkes clearly showed the importance of acid–base interactions on the adsorption of polymers onto solid

* Corresponding author.
E-mail address: benzarti@lcpc.fr (K. Benzarti).

0008-8846/$ - see front matter © 2005 Elsevier Ltd. All rights reserved.
doi:10.1016/j.cemconres.2005.02.005

surfaces [3]. He suggested that the reversible work of adhesion has additive dispersive and acid–base interaction components. The London dispersive interactions are ubiquitous (always present between materials in interaction) whereas the Lewis acid–base interactions (this term includes hydrogen bonds and Bronsted acid–base interactions) occur only when an acidic species is in close contact with an antagonist basic one.

The acid–base properties of materials, such as polymers, metal oxides, fillers, fibres, inorganic substrates can be investigated using various techniques, including microcalorimetry [4], micro-gravimetric analysis [5], contact angle measurements [6], infra-red spectroscopy [7], nuclear magnetic resonance [8], X-ray photoelectron spectroscopy (XPS) [9], ellispometry [10] and inverse gas chromatography (IGC) [11]. Inverse gas chromatography is now a well-established technique for the determination of the surface thermodynamic properties, including London (i.e. dispersive) and Lewis acid–base (i.e. polar) interactions, at the molecular level [12]. It has been proved that this technique is very effective for the characterisation of the surface thermodynamic energy of various finely divided powders, such as conventional polymers [13–15], conducting polymers [16], metal oxides [17], silica [18], surface-modified alumina [19], surface-oxidised glass [20,21] and carbon fibres [22,23], mineral fillers used in paint industry [24] and in rubber mixtures [14,15]. The main advantage of IGC is the determination of the surface thermodynamic properties of divided materials over a wide range of working temperatures and the large set of molecular probes that can be used to characterise the materials under test.

Of relevance to the present work, IGC-ID has been widely used for the characterisation of the surface thermodynamic properties of various clays and hydrated materials such as smectites [25], kaolinites and illites [26], sepiolite [27], talc [28,29] and montmorrillonite [30], depending on the surface chemical composition, geometrical structure of the mineral sheets and thermal pre-treatments before analysis.

Recently, Oliva et al. reported for the first time the characterisation of the surface energy of hardened cement pastes by inverse gas chromatography at infinite dilution [31]. The surface thermodynamic properties of these materials were correlated with the surface elemental compositions as determined by X-ray photoelectron spectroscopy (XPS) [32]. This study demonstrated that the compounds under investigation are fairly high surface energy materials as judged by the respective dispersive contribution to the surface free energy (γ_s^d), and that they exhibit amphoteric properties, with a predominantly basic character. This work also clearly demonstrated significant changes of the surface energy and surface composition induced by coating of the cement pastes with an epoxy resin or a hardener. Particularly, the aminated hardener of the epoxy resin, namely triethylene tetramine (TETA) was found to considerably minimize the surface free energy values of the cement pastes. This has been attributed to specific hydrogen bonding between the materials and the amine, on the basis of the examination of the nitrogen high-resolution XPS signal.

This work is part of our ongoing program on the characterisation of the surface energy of hardened cement pastes, in connection to bulk physico–chemical properties, such as composition, structure and morphology. This program includes the characterisation of individual components, such as constitutive hydrates and fillers, in order to evaluate their contributions to the overall surface behaviour of hardened cement pastes, and predict interactions with polymer adhesives. For this reason it is fundamentally important to probe the molecular interactions that are likely to occur at the interfaces, since they are related to the interfacial energies.

In this study, the surface thermodynamic properties of three cementitious compounds and a mineral filler, have been investigated by IGC-ID, which is a powerful technique for the characterisation of pulverulent or powdery materials. The materials under test are, namely: calcium hydroxide ($Ca(OH)_2$), ettringite ($3CaO{\cdot}Al_2O_3{\cdot}3CaSO_4{\cdot}32H_2O$) and calcium-silicate-hydrate (C-S-H), respectively, and the mineral filler is calcium carbonate ($CaCO_3$). Experiments have been carried out at 35 °C in order to be as close as possible to practical implementation of cement mixtures in construction. Moreover, in the case of hydrated components (i.e. ettringite and C-S-H), additional characterisations of the surface thermodynamic properties have been carried out at increasing working temperatures in order to determine the influence of water content, either adsorbed onto the surface or contained in the structure of hydrates. Thermogravimetric analyses (TGA) provided monitoring of the overall water loss as a function of temperature.

Additional characterisations have been carried-out by X-ray photoelectron spectroscopy (XPS), in order to assess the elemental composition at the surface of samples. XPS is often associated to IGC experiments [16,21,31,32], since the two techniques provide complementary information and give an insight into the relationship between the actual surface composition and the surface energetics of the materials under test.

2. Experimental section

2.1. Cement components

The three cement compounds characterised in this work are calcium hydroxide (i.e. $Ca(OH)_2$ or portlandite), calcium-silicate-hydrate (C-S-H) and ettringite (i.e. $C_3A{\cdot}3CaSO_4{\cdot}32H_2O$). They were prepared at the Laboratoire Central des Ponts et Chaussées (Paris, France) according to standard procedures [33], which are detailed in Appendix A. The identities and purities of these products were controlled by X-ray diffraction analyses (XRD). The materials were analysed without additional treatment, and the various

characterisations (TGA, BET, XPS, IGC) were performed exclusively on fresh and virgin samples.

The mineral filler (calcite, $CaCO_3$) is a natural marble powder provided by Prolabo (France, 99% purity).

2.2. Thermogravimetric analysis (TGA)

Thermogravimetric analyses were carried out with a NETZSCH STA 409C instrument. The samples (20–30 mg) were heated from room temperature up to 1150 °C, with a scan rate of 10 °C min^{-1}, and under an air atmosphere stream (air flow = 80 ml min^{-1}) to ensure water desorption. The residue is assumed to be dehydrated inorganic material. The samples were analysed as received (i.e. without any vacuum pre-treatment or special heat conditioning).

2.3. Specific surface area measurements (BET)

Specific surface area (A_s) was measured with a Micromeritics Model ASAP 2010, using the BET specific surface area procedure of adsorption–desorption cycles of nitrogen. The samples (20–40 mg) were cooled down to liquid nitrogen under a flow of N_2 and were then heated up to room temperature. The amount of desorbed nitrogen was measured by a thermoconductivity detector and allowed to determine A_s for each sample. Each sample was outgassed under vacuum overnight before analysis.

2.4. X-ray photoelectron spectroscopy (XPS)

XPS analyses were performed using a Thermo VG Scientific ESCALAB 250 spectrometer. The instrument is equipped with a microfocusing monochromatic AlKα X-ray source ($h\nu = 1486.6$ eV), high transmission efficiency spectrometer, magnetic lens and a six channeltron detector system. Uniform charge compensation was achieved using both electron and argon flood guns [34]. Analyses were performed with a spot size of 650 μm diameter. The pass energy was set at 150 and 50 eV for the survey and the high resolution spectra, respectively. Data acquisition and processing were achieved with the supplier's Avantage software, version 1.85. Surface compositions were calculated using the peak areas of the specific high resolution spectra (after Shirley background subtraction) and the corresponding manufacturer's sensitivity factors.

Before XPS analyses, each sample was vacuum dried in a dessiccator overnight, mounted on a powder holder, and outgassed in the preparation chamber of the equipment at $\sim 10^{-8}$ mBar.

2.5. Inverse gas chromatography at infinite dilution (IGC-ID)

A Hewlett Packard HP 6890 gas chromatograph was used to determine the surface thermodynamic properties of the cement paste components. This equipment is fitted with a flame ionisation detector (FID) and an electronic flow control system (EFC). High purity nitrogen was used as the carrier gas, with a flow rate set at 25 ml min^{-1}. For the FID detector, a high signal to noise ratio was obtained using high purity hydrogen gas cylinder (flow rate set up at 30 ml min^{-1}) and compressed air fitted with moisture and hydrocarbon removal cartridges (flow rate set up at 300 ml min^{-1}). The injector and detector temperatures were set at 100 and 150 °C, respectively. The chromatograms were collected with a Borwin acquisition system (version 1.21), and the retention times were determined at the peak maxima. All IGC experiments were carried out at 35 °C for all materials. In the case of ettringite and C-S-H, additional characterisations were performed at 60, 90 and 120 °C.

Before column packing, the materials were pellet-pressed, then ground and finally sieved to give the diameter

Table 1
Suppliers and physico–chemical properties of the molecular probes used in this work[a]

Molecular probe	Abbreviation	Supplier purity (%)	Bp (°C)	DN (kJ mol^{-1})	AN* (kJ mol^{-1})
n-Pentane	*n*-C5	Prolabo (+99.0%)	36.1	–	–
n-Hexane	*n*-C6	Prolabo (+99.0%)	69.0	–	–
n-Heptane	*n*-C7	Acros (+99.0%)	98.4	–	–
n-Octane	*n*-C8	Fluka (+99.0%)	125.7	–	–
n-Nonane	*n*-C9	Fluka (+99.0%)	150.8	–	–
n-Decane	*n*-C10	Fluka (+99.0%)	174.1	–	–
Dichloromethane	CH_2Cl_2	Prolabo (+99.0%)	40.0	0	16.3
Chloroform	$CHCl_3$	Prolabo (+99.0%)	61.7	0	22.6
Carbon tetrachloride	CCl_4	Prolabo (+99.0%)	76.8	0	0.7
Diethyl ether	Ether	Merck (+99.0%)	35.0	80.3	5.9
Methyl acetate	Me-Ac	Prolabo (+99.0%)	57.0	69.0	6.7
Tetrahydrofuran	THF	Prolabo (+99.0%)	67.0	83.7	2.1
1-Pentene	1-π5	Aldrich (+99.0%)	30.0	–	–
1-Hexene	1-π6	Aldrich (+99.0%)	63.3	–	–
1-Heptene	1-π7	Aldrich (+99.0%)	94.0	–	–
Benzene	Benz	Prolabo (+99.0%)	80.0	0.1	0.17

[a] BP, DN and AN* are respectively the boiling temperature and the Gutmann's donor and acceptor numbers.

size in the 250–400 μm range which is adequate for GC measurements. Stainless steel columns (3 mm outer diameter and ca 35 cm long) were filled with 0.8–1.2 g of the minerals under test. Prior to chromatographic measurements, the columns were conditioned overnight at the working temperature under a nitrogen gas stream.

Methane was used as a non-interacting marker for the determination of the column dead time. A range of non-polar, Lewis acidic and basic molecular probes (see Table 1) were used to determine the surface thermodynamic properties of the solid materials. The probe vapours were injected manually, at least in triplicate, by an SGE gas-tight syringe. To achieve extreme dilution of the probes, the syringe was purged as many times as necessary, and thus the signals were recorded at the detection limit of the GC equipment. The retention times were averaged over the number of injections.

3. IGC theory

3.1. Adsorption behaviour of molecular probes in inverse gas chromatography

In inverse gas chromatography (IGC), the term *inverse* means that the stationary phase packed into the chromatographic column is of interest in contrast to conventional gas chromatography (GC), where the injected gas mixture is the system under investigation. Injection of molecular probes of known physico–chemical properties allows one to characterize the surface thermodynamic properties of the packed material. The molecular probes are injected at infinite dilution in order to rule-out lateral probe–probe interactions and favour probe-stationary phase (gas–solid) interactions only. The probe undergoes reversible adsorption–desorption cycles. The surface partition coefficient K_s of a probe between the mobile phase (carrier gas) and the stationary phase (solid) is expressed by:

$$K_s = V_N/A \tag{1}$$

where V_N is the net retention volume and A is the total surface area of the stationary phase.

The net retention volume V_N is related to the net retention time t_N of the injected molecular probe by:

$$V_N = j \times F \times t_N = j \times F \times (t_R - t_0) \tag{2}$$

where j is the gas compression correction factor, F is the corrected carrier gas flow rate, t_R is the retention time of the molecular probe and t_0 is the retention time of a non-sorbed species (i.e. methane marker), respectively. The net retention volume V_N stands for the volume of carrier gas needed to sweep out the injected probe through the stationary phase column. The higher is the affinity of the injected molecular probes towards the stationary phase under investigation, the higher is the retention time and thus V_N.

Since K_s is an equilibrium constant, one can determine the standard free energy required to transfer a mole of vapour from the gas phase to a standard state on the stationary phase surface using the following equation:

$$-\Delta G^{ads} = RT\cdot\ln(V_N) + C \tag{3}$$

where R is the gas constant, T is the column temperature during IGC experiment and C is a constant that takes into account the weight and the surface area of the stationary phase and the reference standard states of the probe in the mobile and adsorbed phases [35].

The interaction energy at the absorbent–adsorbate interface can be split into dispersive (ΔG^d) and specific (ΔG^{spec}) components:

$$\Delta G^{ads} = \Delta G^d + \Delta G^{spec} \tag{4}$$

The IGC determination of the free energy of adsorption (ΔG^{ads}) values for a series of non-polar linear alkanes and also specific molecular probes interacting through Lewis acid–base interactions, will yield the determination of the dispersive (London interactions) and specific (Lewis acid–base interactions) contributions to the surface energy of the stationary phase, respectively. According to Fowkes, the total surface free energy of a solid material (γ_s) has two additive dispersive (γ_s^d) and specific (γ_s^{spec}) components (i.e. $\gamma_s = \gamma_s^d + \gamma_s^{spec}$) [1,2].

3.2. Dispersive interactions

For solid materials, London dispersive interactions are usually described by γ_s^d, the dispersive component of the free surface energy. A standard method by IGC to determine γ_s^d of the stationary phase relies on the use of a series of linear alkane molecular probes. It is well known that for the latter series, the plot of ($-\Delta G^{ads}$) values versus the number of carbon atoms n_c, results in a linear correlation. The slope of the straight line corresponds to the free energy of adsorption of a methylene group ($-\Delta G^{CH2}$). Dorris and Gray [36] proposed that the dispersive free energy component (γ_s^d) of the stationary phase be related to the free energy of adsorption of a methylene group by:

$$\gamma_s^d = \left(\frac{1}{4\cdot\gamma_{CH2}}\right)\cdot\left(\frac{-\Delta G^{CH2}}{N\cdot a_{CH2}}\right)^2 \tag{5}$$

where N is the Avogadro's number, a_{CH2} is the cross sectional area of an adsorbed methylene group (a_{CH2}=6 Å^2) and γ_{CH2} is the surface free energy of a solid material constituted by methylene groups only, such as polyethylene [γ_{CH2}=36.8–0.058 T (T is the working temperature, in °C)].

3.3. Lewis acid–base interactions

Since only the total retention volume is determined in IGC, Eq. (3) can only yield the total free energy of adsorption from the retention data. It is therefore necessary

to apply appropriate methods to distinguish the dispersive from the specific contributions to the total free energy of adsorption using the retention data. Several quantitative approaches have been suggested to distinguish between the London dispersive contribution and Lewis acid–base interactions, and thereby deduce acid–base parameters for the stationary phase under test. Methods have been developed by Brookman and Sawyer [37], Saint Flour and Papirer [38], Koning et al. [39], Shultz and Lavielle [40], Osmont and Schreiber [41], Donnet et al. [42], Tiburcio and Manson [43] and Chehimi and Pigois-Landureau [44]. The advantages and limitations of these methods have been discussed in the literature [45].

In this study, in order to evaluate the specific adsorption energy (ΔG^{spec}) from the total adsorption energy (ΔG^{ads}), we relied on the approach of Brookman and Sawyer [37], in which, ΔG^{ads}, or simply ($RT\cdot \ln V_N$), values are plotted against the boiling temperatures (T_b, in °C) of the molecular probes injected. The *n*-alkane series leads to a linear plot, which constitutes a reference straight line for the London dispersive interactions. For Lewis probes, able to adsorb through acid–base interactions with the stationary phase, $-\Delta G^{ads}$ values are expected to deviate above the linear correlation defined by the *n*-alkanes probes. Assuming that dispersive and acid–base interactions are additive (see Eq. (4)), the specific contribution to the free energy of adsorption (ΔG^{spec}) is easily calculated from the total free energy of adsorption (ΔG^{ads}). For the Lewis molecular probe, ΔG^{spec} corresponds to the vertical distance between the $-\Delta G^{ads}$ value and the reference line defined by the *n*-alkanes series, according the following equation:

$$\begin{aligned}\left(-\Delta G^{spec}\right) &= \left(-\Delta G^{ads}\right) - \left(-\Delta G^{ref}\right) \\ &= RT\cdot\ln\left(V_{N,\,Lewis}/V_{N,\,ref}\right)\end{aligned} \quad (6)$$

where $V_{N,\,Lewis}$ and $V_{N,\,ref}$ refer, respectively, to the retention volumes of the Lewis probe and a hypothetical reference *n*-alkane probe having similar boiling point [37].

If the stationary phase exhibits an amphoteric character, both Lewis acidic and basic molecular probes will lie significantly above the reference *n*-alkane line.

4. Results and discussion

4.1. X-ray photoelectron spectroscopy (XPS)

Fig. 1 shows the XPS survey spectra of calcium hydroxide, calcium carbonate, ettringite and C-S-H, respectively. The elemental surface compositions of the materials, as determined by XPS, are reported in Table 2.

For all specimens, oxygen (O_{1s} at ~530 eV and O_{KLL} at ~980 eV) and calcium (Ca_{2s} at ~440 eV and Ca_{2p} at ~350 eV) signals are clearly detected. The presence of these elements was expected and is consistent with the theoretical bulk chemical composition of the compounds.

In addition, carbon (C_{1s} at ~285 eV) and magnesium (Mg_{KLL} at ~300 eV) species are also detected. The origin of the carbon content will be discussed in the next paragraph. The magnesium content may be attributed to impurities of the raw materials that were used in the synthesis procedures (i.e., calcium carbonate, etc...). However, the significant Mg content found at the surface of portlandite (5.8 at.%) is quite unexpected and still not explained.

In the case of calcium carbonate, the detection of silicon (Si_{2p} and Si_{2s} signals centred at ~103 and 155 eV, respectively) could be an indication that the marble powder under test contains natural impurities such as quartz or other silica forms. On the contrary, a silicon content was expected in the C-S-H, since this element is present in the bulk material: $Ca_3(OH)_2(H_2SiO_4)_2$. It should be noticed that X-ray diffraction analyses were performed on the different batches and that the actual presence of a C-S-H phase was confirmed. Additionally, XPS data provide a C/S ratio of 0.7, which differs significantly from the C/S ratio of 1.5 assessed by inductively coupled plasma spectroscopy (ICP) on the bulk material [33]. This feature suggests that the silicon content is higher at the extreme surface of C-S-H than in the bulk. Further results regarding the XPS characterisation of C-S-H are available in the literature [46–48].

For ettringite, additional sodium (Na_{1s} at ~1072 eV and Na_{KLL} at ~500 eV), sulphur (S_{2p} at ~165 eV and S_{2s} at ~230 eV) and aluminium (Al_{2p} at ~75 eV and Al_{2s} at ~120 eV) species are also detected.

Fig. 2 displays the carbon C_{1s} signals for calcium hydroxide (Fig. 2a), calcium carbonate (Fig. 2b), ettringite (Fig. 2c) and C-S-H (Fig. 2d). The C_{1s} regions exhibit two main peaks. The first peak is centred at 285.0 eV and can be assigned to aliphatic carbon species coming from an adventitious carbon contamination. Such a contamination is quasi un-avoidable and found on most organic and inorganic surfaces, due to oily vapours and dusts that are naturally present in the ambient environment. Because the contamination affects the surface of materials it is readily detected by XPS, especially in the case of high surface energy materials such as metals and metal oxides. The second peak centred at 289.6±0.2 eV, can be assigned to carbonate species at the materials' surfaces. It is an indication that the materials have been slightly carbonated during the preparation or the conditioning, due to the adsorption of CO_2 from the atmosphere. This will be confirmed by TGA analyses in the next section. For calcium carbonate, the high binding energy peak is more intense than the peak corresponding to aliphatic species, as obviously expected from the chemical structure of this inorganic compound.

4.2. Thermal analysis

Thermogravimetric analysis (TGA) was used in order to evaluate the overall water content, accounting both for

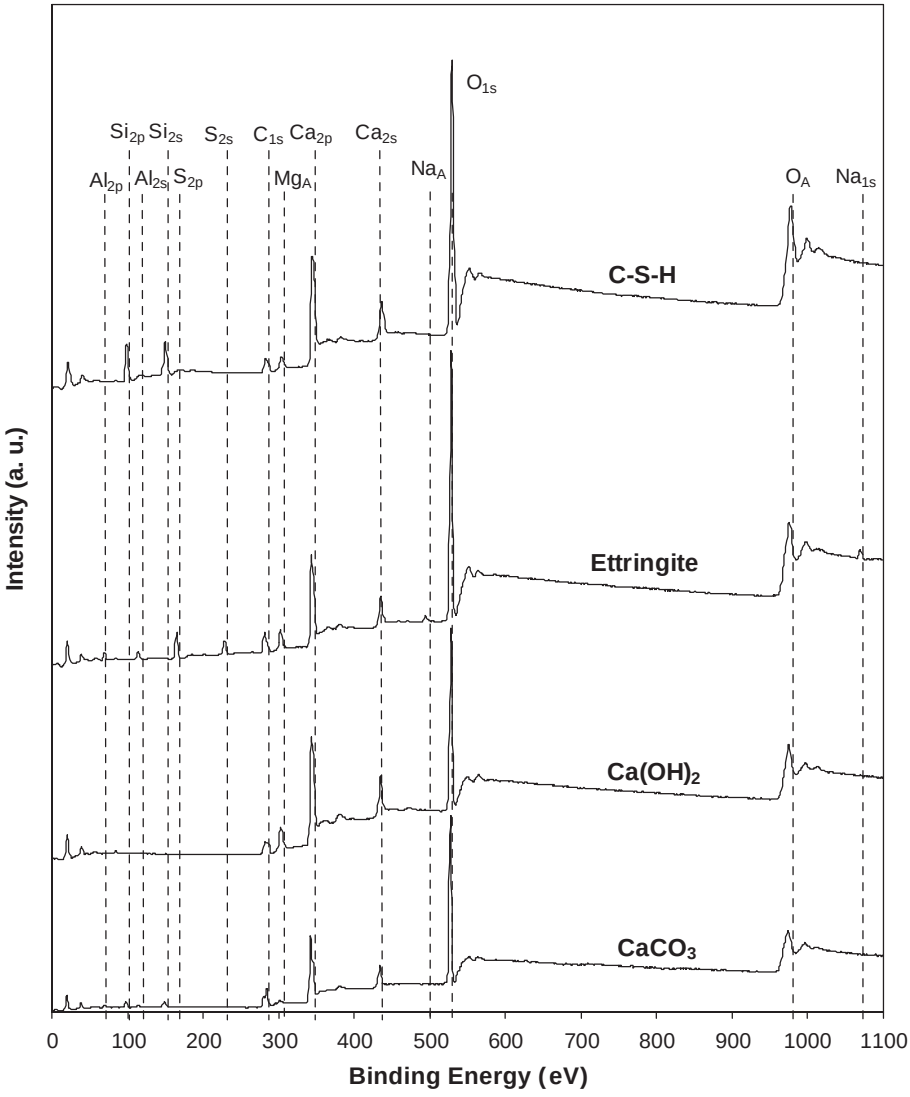

Fig. 1. XPS survey spectra of the various materials under test, and assignments of the main peaks.

adsorbed and structural water, the contributions of which cannot be differentiated.

Fig. 3 displays the weight losses with temperature for the various materials. The overall weight losses (in percent) observed up to 600 °C and after complete thermal treatment at 1100 °C are reported in Table 3 for the various compounds. At 600 °C, most of the water has been released, and the weight loss is quasi-representative of the overall water content. Therefore we have assumed that the additional weight loss between 600 and 1100 °C, is mainly due to the release of CO_2 associated to carbonation (see explanations below).

Table 2
Elemental surface composition (in at.%) as determined by X-ray photoelectron spectroscopy (XPS)

	Calcium hydroxide	Calcium carbonate	Ettringite	C-S-H
C (total content)	14.9	22.6	11.6	7.7
N	–	–	Traces	–
O	56.1	54.7	55.8	56.3
Ca	23.2	16.2	14.0	14.0
Mg	5.8	0.9	2.9	2.1
Si	–	5.6	Traces	20.0
Al	–	–	6.2	–
S	–	–	8.3	–
Na	–	–	1.3	–

TGA analyses clearly reveal differences in thermal behaviour between the analysed materials.

Calcium carbonate is relatively stable with thermal treatment and does not exhibit any weight loss up to 650 °C, which indicates a very low water content. At higher temperatures, the weight loss is mainly due to the release of carbon dioxide due to the decomposition process described by:

$$CaCO_3 \xrightarrow{\Delta} CaO + CO_2 \quad (7)$$

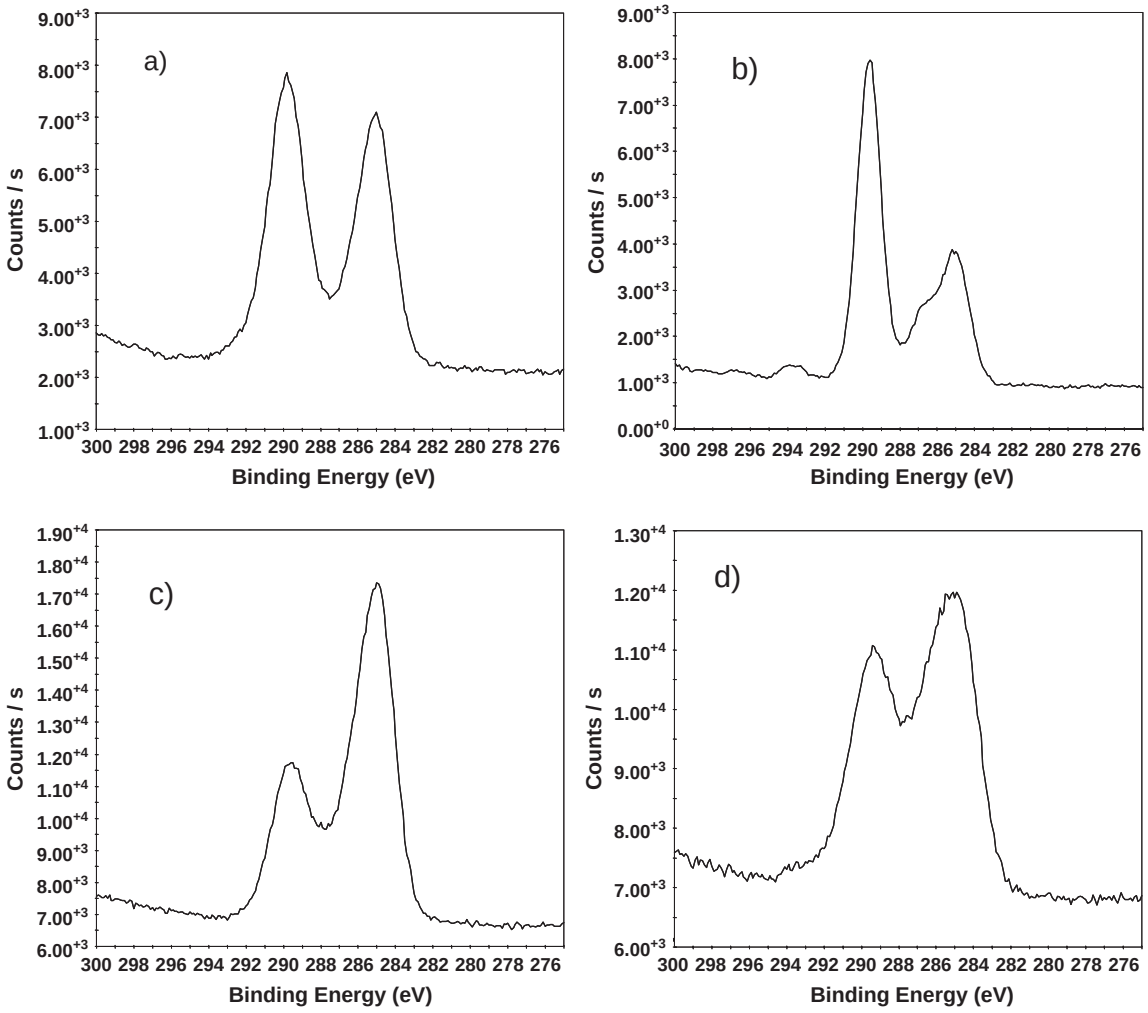

Fig. 2. XPS high-resolution C1s spectra of: (a) calcium hydroxide, (b) calcium carbonate, (c) ettringite and (d) C-S-H.

Calcium hydroxide exhibits a major weight loss around 450 °C, due to the release of water molecules coming from the condensation of adjacent hydroxyl groups (see Eq. (8)). An additional weak weight loss is observed around 650 °C, due to the release of CO_2, and showing that the surface of portlandite has been slightly carbonated prior to the TGA

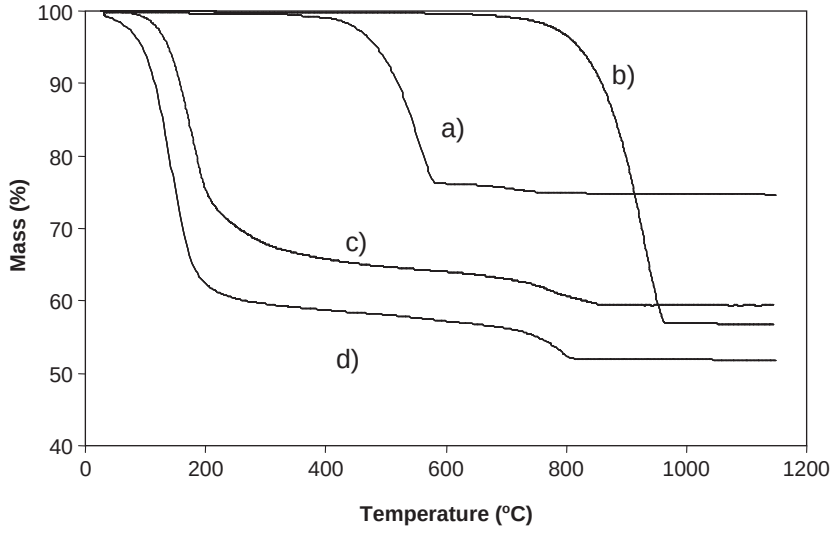

Fig. 3. Thermogravimetric analysis curves (weight loss vs. temperature) for (a) calcium hydroxide, (b) calcium carbonate, (c) ettringite and (d) C-S-H.

Table 3
Weight loss (in percent) to 600 and 1100 °C, and specific surface area (A_S, in $m^2\ g^{-1}$) of the materials as determined by thermogravimetric analysis (TGA) and BET measurements respectively

Cement component	Weight loss (%) at:		Specific surface area ($m^2\ g^{-1}$)
	600 °C	1100 °C	
Calcium hydroxide	23.8	25.3	7.9
Calcium carbonate	0.3	43.2	2.6
Ettringite	36.0	40.6	20.8
C-S-H	42.8	48.1	180.7

characterisation (see Eq. (9)). This is a confirmation of the previous observations by XPS.

$$Ca(OH)_2 \xrightarrow{\Delta} CaO + H_2O \quad (8)$$

$$Ca(OH)_2 + CO_2 \rightarrow CaCO_3 + H_2O \quad (9)$$

Ettringite and C-S-H exhibit a completely different behaviour: most of the water loss (both adsorbed and structural water) occurs at relatively low temperatures, in the 120–400 and 80–250 °C intervals for ettringite and C-S-H, respectively. A continuous but limited water loss is observed at higher temperature and mainly up to 600 °C. Another significant weight loss is observed between 600 and 900 °C. As previously mentioned, we assume that this phenomenon is due to the release of CO_2 and reveals the existence of a substantial surface carbonation.

Globally, ettringite and C-S-H exhibit the highest weight losses among the four tested compounds, which is consistent with the hydrated nature of these materials.

4.3. Specific surface area measurements

The specific surface area A_S of the compounds has been determined by BET measurements. The values of A_S are also reported in Table 3. The specific surface area, A_S, varies depending upon the structure of the materials. Calcium hydroxide and calcium carbonate are low specific surface area materials, whereas C-S-H exhibits a very high specific surface area. This result clearly demonstrates that the porosity and lamellar sheet structure varies depending on the nature of the component under investigation.

4.4. Surface energy characterisation

The surface energy (dispersive and acid–base properties) of the cement components have been investigated by IGC-ID using a series of non-polar (*n*-alkanes series), Lewis acidic and basic, and aromatic molecular probes at 35 °C. This temperature is representative of actual implementation conditions of cementitious materials in civil engineering.

4.4.1. Evaluation of dispersive properties

A typical gas chromatogram obtained for ettringite at 35 °C is shown in Fig. 4. This figure illustrates the difference in retention time, when a mixture of *n*-alkane probes (*n*-C5, *n*-C6 and *n*-C7) is injected simultaneously within the column. Methane is the non-interacting probe, and defines the zero retention time (i.e. injection time). The retention times of the *n*-alkane probes increase as the number of carbon atoms in the chain increases. Similar chromatograms were obtained for the other materials.

Fig. 5 shows a plot of $RT\cdot\ln(V_N)$ versus the number of carbon atoms n_c in the alkane chain, as determined at 35 °C for calcium hydroxide, calcium carbonate, ettringite and C-S-H, respectively. For all specimens under test, excellent linear correlations of $RT\cdot\ln(V_N)$ vs. n_c are generated for the *n*-alkane series. As mentioned in Section 3.2, the slope of the straight line corresponds to the free energy of adsorption of a methylene group ($-\Delta G^{CH2}$). This increment permits to determine the dispersive contribution to the free energy (γ_s^d) of the stationary phase using Eq. (5). Table 4 reports

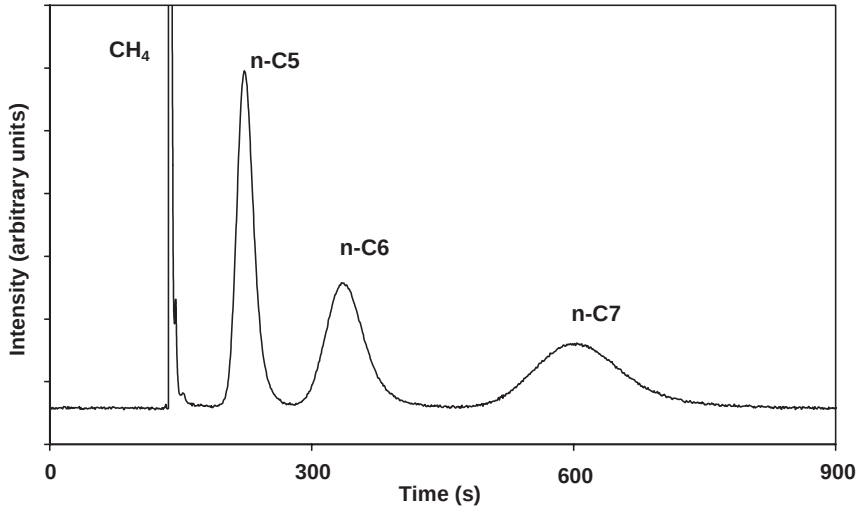

Fig. 4. Typical gas chromatogram showing output signal following the injection of a mixture of *n*-alkane probes (n-C5, n-C6, n-C7) obtained for ettringite at 35 °C. The methane probe is assumed to have a zero retention time and provides the calibration point for the determination of the net retention times.

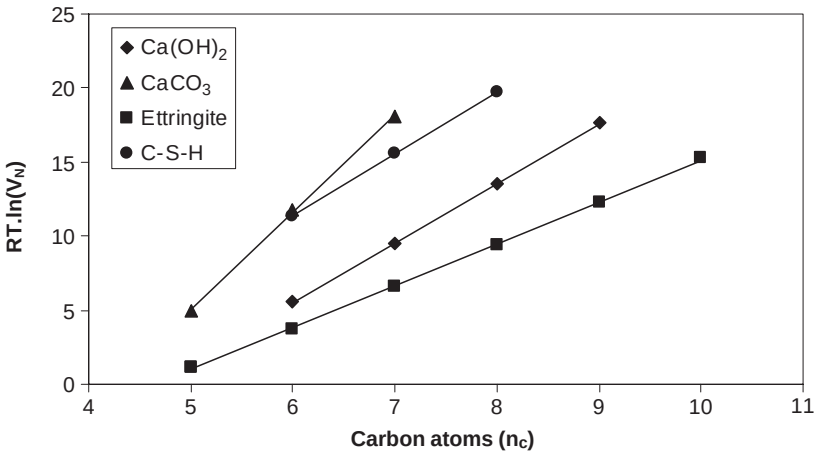

Fig. 5. Plot of $RT\cdot \ln(V_N)$ versus the number of carbon atoms n_c for n-alkane series determined for the various materials at 35 °C.

$(-\Delta G^{CH2})$ and γ_s^d values determined at 35 °C for the various compounds. In the case of hydrated materials, ettringite and C-S-H, Table 4 also reports additional determinations of the $(-\Delta G^{CH2})$ and γ_s^d values at 60, 90 and 120 °C, respectively.

At 35 °C, the γ_s^d values decrease in the following order:

$$CaCO_3 > C-S-H > Ca(OH)_2 > \text{Ettringite}$$

This trend demonstrates that the nature, the structure and the chemical composition of these compounds significantly affect their surface dispersive properties. There is also a good correlation between these properties and the water content of the materials as determined by TGA. Indeed, the higher the water content, the lower the dispersive contribution to the free energy (γ_s^d) at 35 °C, except for C-S-H.

Nevertheless, for C-S-H and ettringite activated overnight and characterised at 120 °C, γ_s^d values are rather constant, whereas the water content is significantly decreased, as demonstrated by TGA.

It is interesting to note that Oliva et al. [31] reported γ_s^d values for cement pastes (in the 50–70 mJ/m^2 range at 35 °C) that are in line with those reported in Table 4 for the individual cement paste components, especially C-S-H and ettringite. These are medium to fairly high values that clearly demonstrate that the cement pastes and their components and/or additives behave as high surface energy materials, especially calcium carbonate. Indeed, for $CaCO_3$, this result is in good agreement with the work previously reported by Keller and Luner [49]. These authors showed that thermal treatment of $CaCO_3$ before analysis induced significant increase of the dispersive contribution up to 250 mJ m^{-2}. It is interesting to note, that for other published results, γ_s^d values for $CaCO_3$ are as low as 44.6 mJ m^{-2} at 30 °C [50]. However γ_s^d values depend on the nature, origin and surface composition of the calcium carbonate powders.

In contrast, ettringite exhibits a quite low γ_s^d value at 35 °C. This low γ_s^d value could be correlated to the high water content of the material. For this reason, the γ_s^d values has been monitored at various working temperatures (up to 120 °C). Increasing the working temperature from 35 to 60 °C leads to significant increase of the γ_s^d value (ca. 10 mJ m^{-2}), due to the desorption of water molecules from the surface. Such an increase of the γ_s^d value with working temperature was also observed by Oliva et al. [31] for hardened cement pastes. Further increase of the working temperature leads however to a slight decrease of the γ_s^d values of ettringite, which may result from a growing degradation of the hydrate structure.

Even though C-S-H material has the highest water content, it exhibits a completely different behaviour compared to that of ettringite. Indeed, C-S-H is characterised by a relative high γ_s^d value. This result can be explained by the different surface composition as determined by XPS and/or due to the very high specific surface area (A_S) of the powder as determined by BET. This highly hydrated material has been also characterised at increasing working temperature. As previously observed for ettringite, an increase of the working temperature leads to a slight increase of the γ_s^d value between 35 and 60 °C, then a slight decrease of the γ_s^d values is measured.

Changes in the γ_s^d values, observed with temperature for ettringite and C-S-H materials, are closely related to the

Table 4
Free energy of adsorption of a methylene group ($-\Delta G^{CH2}$, in kJ mol^{-1}) and dispersive contribution to the total surface energy (γ_s^d, in mJ m^{-2}) as determined by IGC-ID for the analysed materials

Components	Calcium hydroxide	Calcium carbonate	Ettringite				C-S-H			
Temperature (°C)	35	35	35	60	90	120	35	60	90	120
$-\Delta G^{CH2}$ (kJ mol^{-1})	4.0	6.6	2.9	3.1	2.9	2.7	4.2	4.2	4.0	3.7
γ_s^d (mJ m^{-2})	89.6	236.0	45.6	54.4	52.2	48.3	96.3	99.2	96.8	88.6

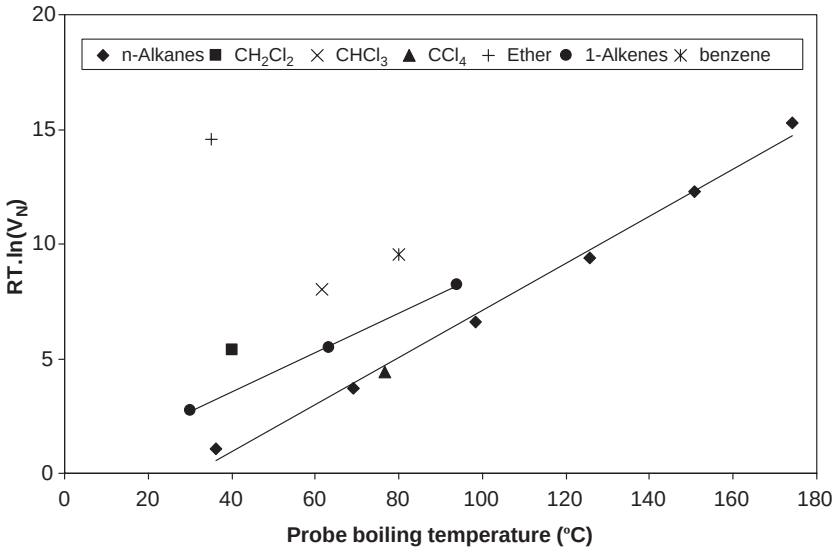

Fig. 6. Plot of ($RT\cdot \ln(V_N)$) versus boiling temperature (°C) of the *n*-alkanes series and Lewis acid–base and aromatic molecular probes injected, obtained for ettringite at 35 °C.

desorption of water molecules up to 60 °C, and may be related to both water desorption and structural degradation of hydrates over 60 °C.

4.4.2. Evaluation of acid–base properties

The acid–base properties of the four compounds have been evaluated using Brookman and Sawyer's approach [37]. Fig. 6 shows a plot of $RT\cdot\ln(V_N)$ vs. boiling temperature (T_b, in °C) of the molecular probes injected into an ettringite-packed column at 35 °C. Similar plots are obtained for the other materials. An excellent linear correlation of $RT\cdot\ln(V_N)$ vs. T_b is obtained for the *n*-alkane series. This straight line defines the reference London dispersive interactions. In contrast, all the Lewis acidic and basic, and aromatic molecular probes markers lie above the reference *n*-alkane line. This observation clearly indicates that additional specific interactions occur between the stationary phase and the specific probes injected. The difference between $RT\cdot\ln(V_N)$ determined for the polar probes and the reference *n*-alkane straight line accounts for $-\Delta G^{spec}$ values according to Eq. (6).

Table 5 reports the $-\Delta G^{spec}$ values determined for the Lewis acidic and basic species and the aromatic molecular probes for the various materials at indicated working temperature. Both Lewis and aromatic molecular probes strongly interact with the stationary phase via specific interactions as judged by the high $-\Delta G^{spec}$ values, hence the amphoteric behaviour of these minerals.

For dichloromethane and chloroform acidic probes, $-\Delta G^{spec}$ values could be determined for all materials. However, among the basic Lewis probes, diethyl ether was the only one which gave a measurable retention time. Attempts to determine retention times for other references Lewis base probes, such as methyl acetate and tetrahydrofuran probes, were unsuccessful due to a very strong adsorption of these probes onto the stationary phases. These results show that basic probes interact strongly or may be absorbed irreversibly onto the stationary phases, and thus indicate a predominant acidic character of these materials.

To overcome this problem, aromatic probes, which exhibit a weak basic character (they are π electron donors) have been used to assess the solid surface acidic characters.

Table 5
Specific contribution to the free energy of adsorption ($-\Delta G^{spec}$, in kJ mol^{-1}) as determined with the acidic and basic probes for the various compounds

Component		Calcium hydroxide	Calcium carbonate	Ettringite				C-S-H			
Temperature (°C)		35	35	35	60	90	120	35	60	90	120
$-\Delta\ G^{spec}$ (kJ mol^{-1})	CH_2Cl_2	4.0	2.5	5.1	6.12	7.3	7.4	5.2	5.6	5.8	6.8
	$CHCl_3$	4.6	−0.4	5.3	5.94	6.5	6.6	nd*	3.9	3.8	4.3
	CCl_4	−1.8	−5.6	0.1	0.24	0.8	0.9	−0.5	−1.1	−1.5	−1.0
	Ether	12.6	nd*	15.0	19.0	24.6	27.5	nd*	nd*	nd*	nd*
	1 − π5	nd*	2.9	3.5	3.68	5.3	nd*	3.5	3.6	3.8	4.9
	1 − π6	1.6	2.3	2.6	2.92	4.1	4.7	3.6	3.4	3.3	3.9
	1 − π7	1.0	1.3	2.0	2.42	3.1	3.5	nd*	nd*	nd*	3.3
	Benz	1.4	nd*	4.9	7.29	7.6	7.5	nd*	nd*	nd*	5.1

nd*: $-\Delta G^{spec}$ values were not determined because no retention peaks could be recorded due to a high retention time and/or broad signals.

Retention times could be measured. These probes lie above the *n*-alkane straight line, as expected. These results clearly demonstrate that these probes strongly interact with the cement components even though they exhibit a weak Lewis basic character. For the 1-alkene series, a slight decrease of the $-\Delta G^{spec}$ values is observed as the number of carbon atoms increases in the molecule. This observation has been reported for the characterisation of silica [51,52].

For both Lewis acids (CH_2Cl_2 and $CHCl_3$), the decreasing trend of ΔG^{spec} absolute values is:

$$C-S-H \sim Ettringite > Ca(OH)_2 > CaCO_3$$

This trend is again consistent with the water content as determined by TGA of the compounds.

In the case of the Lewis basic probes, the retention time of diethyl ether could only be measured for calcium hydroxide and ettringite stationary phases. For C-S-H and calcium carbonate, no signal for diethyl ether could be detected. For methyl acetate and tetrahydrofuran, no signal could be detected, thus $-\Delta G^{spec}$ values could not be determined. It should be noted that the $-\Delta G^{spec}$ values measured for diethyl ether are 3–4 times higher than those determined for the acidic Lewis probes. The high $-\Delta G^{spec}$ values and the non-measurable retention time of most of the basic probes clearly demonstrate the predominant acidic character of the analysed materials.

It is interesting to note that the trends of the $-\Delta G^{spec}$ values determined for the Lewis acidic and basic probes follow the opposite trend determined for the dispersive contribution of the free energy (γ_s^d) of the compounds (excluding C-S-H).

The use of aromatic probes, with weaker basic character, are more suitable for the characterisation of the acidic behaviour of the cement components. For the 1-alkene series, the $-\Delta G^{spec}$ values decrease in the following trend (observed at 35 °C):

$$C-S-H \sim Ettringite > CaCO_3 > Ca(OH)_2$$

The inversion of behaviour between calcium carbonate and calcium hydroxide observed for the 1-akenes series and acidic molecular probes in not clear at the present time.

In the similar manner, for hydrated materials (ettringite and C-S-H), the polar properties have been investigated at various working temperatures. Table 5 reports the $-\Delta G^{spec}$ values determined for the Lewis acidic and basic and the aromatic molecular probes at indicated temperature.

It should be noted that for the acidic probes, $-\Delta G^{spec}$ values slightly increase with temperature, whereas, for the basic probes, especially for diethyl ether in the case of ettringite, $-\Delta G^{spec}$ values significantly increase with temperature. These results suggest that the acidic character of ettringite and C-S-H is strongly activated with temperature. This observation correlates also with the increase of the γ_s^d values with temperature, as previously reported. This activation results partially in the desorption of water, which is a reference amphoteric molecule in nature. It follows that the acid–base character of the materials is likely to be affected by their water content.

Because Lewis acidity and basicity scales are independent, it is more convenient to relate the hydratation of the materials under test to an overall acid–base descriptor. By analogy with the theory of van Oss et al. [53] on the acid–base contribution to the specific surface energy γ^{AB}, we suggest to define an "IGC descriptor of γ^{AB}" as follows (Eqs. (10)–(12)):

$$\gamma_{IGC}^{AB} = 2(\alpha \cdot \beta)^{1/2} \tag{10}$$

where

$$\alpha = -\Delta G^{spec}(1-\pi 6) \tag{11}$$

and

$$\beta = -\Delta G^{spec}(CH_2Cl_2) \tag{12}$$

α is a measure of the acidity and β that of the basicity of the materials. Since $-\Delta G^{spec}$ values are in kJ mol^{-1}, it follows that γ_{IGC}^{AB} is in kJ mol^{-1}.

The choice of this parameter is driven by the fact that water is amphoteric in nature and that its content by weight on the surface of the materials must rather be related to an overall acid–base parameter. We have previously related such a parameter to the surface chemical composition of untreated and oxidized carbon fibres [54]. In this context, Fig. 7 displays a plot of the above-defined γ_{IGC}^{AB} values versus the water loss as determined by TGA up to 600 °C. As shown in Fig. 7, the overall acid–base character roughly increases with water content of the material under investigation.

It is also important to discuss the effect of the superficial sample carbonation on the thermodynamic surface properties. Such a carbonation was revealed by XPS for portlandite, C-S-H and ettringite, through the analysis of the C1s spectra (see Section 4.1). It is well known that calcium containing-phases are subjected to carbonation, either during the synthesis procedure or the characterisation, and that concrete surfaces are naturally carbonated in a standard environment. The formation of calcium carbonate may reduce locally the porosity or the specific surface area of the materials, and therefore affect somehow the surface properties. However, since all the compounds are slightly carbonated, the large differences observed in the surface properties (γ_s^d and $-\Delta G^{spec}$ values) should be attributed to the intrinsic behaviours of the materials.

Finally, it is interesting to consider the carbon tetrachloride adsorption behaviour on the mineral surfaces. Since CCl_4 is a weak Lewis acidic molecular probe, the retention data (i.e. $RT \cdot \ln(V_N)$) of this probe should lie on, or slightly above, the reference straight line defined by the *n*-alkane series (as displayed in Fig. 5). However, for this probe, negative $-\Delta G^{spec}$ values were determined (see Table 5) which is rather surprising. This indicates that CCl_4 interacts less energetically than expected with the stationary phase

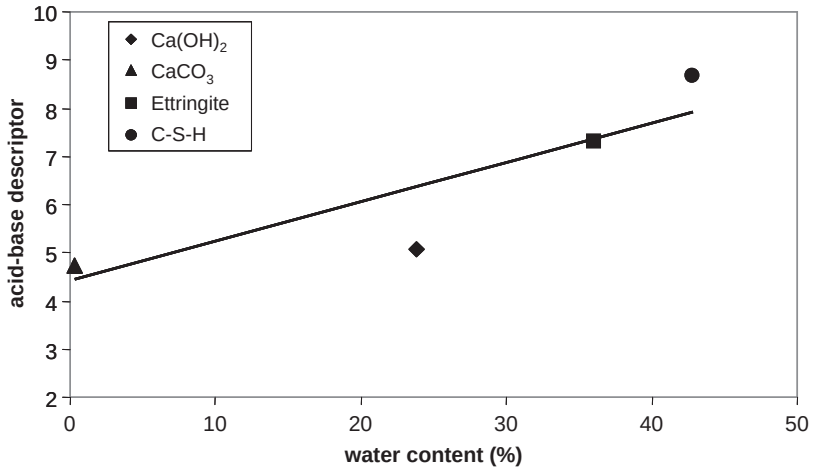

Fig. 7. Graph showing the overall acid–base properties ($2\ (\alpha \cdot \beta)^{1/2}$) as determined by IGC versus the water content (in weight percent) as determined by TGA at 600 °C for the various materials.

materials. The lower retention time measured can be explained by the high volume of the molecule due to the four chlorine atoms (determined using van der Waals volume), and thus this molecule can perhaps not probe all the surface area available. This phenomenon is particularly important in the case of microporous or lamellar materials, where the surface inside the pores is not available for such bulky probes. It is interesting to note that Papirer's research group [26] already reported such negative ($-\Delta G^{spec}$) values for CCl_4 probe in the case of the characterisation of kaolinites and illites by IGC-ID at 140 °C. These observations were not clearly understood and thus no explanations were given to interpret this phenomenon. Fig. 8 displays ($-\Delta G^{spec}$) values versus (γ_s^d) values for the present cement materials and data pertaining to kaolinites and illites [26]. As shown in Fig. 8, a linear decrease of the ($-\Delta G^{spec}$) values is observed with increase of the (γ_s^d) values of the materials under test.

5. Conclusions

The surface thermodynamic properties of three mineral hydrates (namely, $Ca(OH)_2$, C-S-H and ettringite), which are the main components of hardened cement pastes, and one mineral filler ($CaCO_3$ or marble powder) have been characterised by inverse gas chromatography at infinite dilution at 35 °C. This study clearly demonstrates that these materials exhibit different London dispersive components of the surface energy γ_s^d and acid–base properties. Indeed, they are found to be medium to high surface energetic materials as judged by the γ_s^d values, ranging from 45.6 up to 236 mJ m^{-2}. In addition, they exhibit amphoteric properties, with a predominant acidic character, as demonstrated by the strong interactions of the stationary phases with various Lewis basic and aromatic molecular probes. The surface thermodynamic properties have been correlated with the water content of the materials, as determined by thermogravimet-

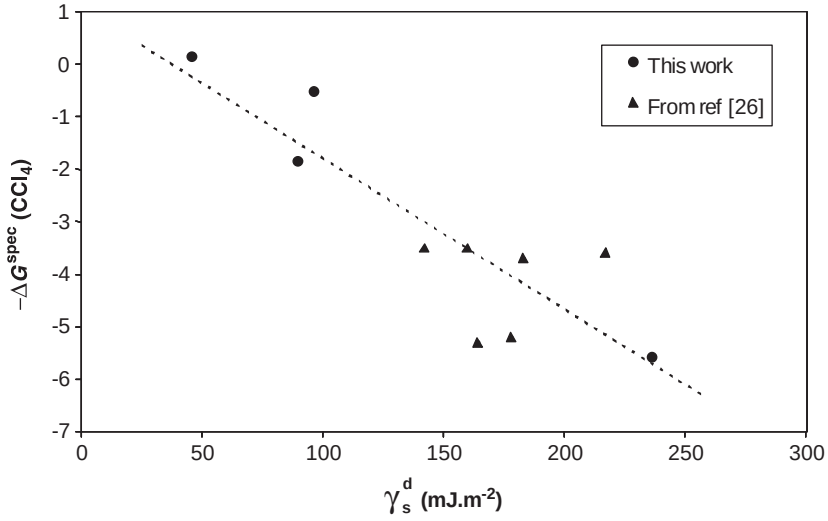

Fig. 8. Graph ($-\Delta G^{spec}$) values versus γ_s^d values obtained for the cementitious components and additional values from Saada et al. [26]. The line of best fit is calculated both from the present experimental results and from the literature data.

ric analysis. The higher the water content, the lower the γ_s^d values. This result is due to the low γ_l^d value of water, still adsorbed on the materials' surfaces at 35 °C. In contrast, the interaction of specific polar probes with these materials is more energetic since water is an amphoteric species in nature. Indeed, the overall acid–base descriptor ($\gamma_{IGC}^{AB}=2\cdot(\alpha\cdot\beta)^{1/2}$) was found to roughly increase with the overall water content of the materials under investigation. Moreover, analyses performed at increasing temperatures clearly demonstrated activation of the mineral surfaces, as judged by the $-\Delta G^{spec}$. This result is interpreted in terms of loss of water molecules, resulting in more energetic interactions between the specific probes and the materials.

XPS experiments also revealed a superficial carbonation of the samples, which may have an additional influence on the surface thermodynamic properties. But all samples are partially carbonated and the large differences observed in the thermodynamical properties of the compounds cannot be explained by this phenomenon.

This IGC study is of fundamental importance for the understanding of the surface thermodynamic properties of mineral compounds, in relation to their properties as components of fully formulated hardened cement pastes.

Acknowledgements

The authors would like to thank the LCPC and University Paris 7 for their financial support (Research project 2002-C027). CP gratefully acknowledges the French Ministry of Education, Research and Technology for an ATER lecturership position. Authors also thank S. Fenouillet, L. Divet, E. Massieu and T. Chaussadent (LCPC) for their contribution to the material synthesis and characterisation.

Appendix A. Synthesis procedures of portlandite, C-S-H, and ettringite

A.1. Preparation of portlandite

Natural marble powder $CaCO_3$ was used as the raw material. The process involved two successive stages, i.e., the fabrication of calcium oxide CaO from calcium carbonate and the transformation of CaO into portlandite:

- In order to prepare the quicklime CaO, a mass M_{CaCO3} of calcium carbonate was poured into a platinum crucible. The mass of the empty crucible was noted M_c. The filled crucible was then placed in a muffle furnace at 1100 °C, for approximately 5 h (time required for the decarbonation of $CaCO_3$, according to the reaction shown in Eq. (7)). When the decarbonation was completed, the mass of the resulting material $M_{CaO}=(M_{TOTAL}-M_c)$ verified the relation $M_{CaO}=0.56\ M_{CaCO3}$,
- In the second step, calcium oxide was placed on the bottom of a glass lens, and boiling water was poured drop by drop on the material, using a syringe or a pipette. Reaction (A.1) led to the formation of portlandite:

$$CaO + H_2O \rightarrow Ca(OH)_2 \quad (A.1)$$

In order to remove the excess of water, the samples were stored at room temperature, in a dessiccator over silica gel.

A.2. Preparation of C-S-H

The synthesis of C-S-H was performed according to the "caustic soda method", and the corresponding reaction is described in Eq. (A.2).

C/S and H/S ratios of the resulting product were respectively equal to 1.57 and 1.26, as derived from ICP experiments (inductively coupled plasma spectroscopy) [33].

$$\begin{aligned}(4Na^+ + 2H_2SiO_4^{2-}) + 6(Na^+ + OH^-) \\ + (10Cl^- + 5Ca^{2+}) \rightarrow (Ca_3(OH)_2(H_2SiO_4)_2) \\ + (2Ca^{2+} + 4OH^-) + 10(Na^+ + Cl^-)\end{aligned} \quad (A.2)$$

The experimental device consisted of an Erlenmeyer flask placed on a magnetic stirrer, and of two separating-funnel filled with the reactive products. The evacuation of each separating-funnel was ensured by a capillary device equipped with a tap. The two capillaries were in contact with the wall of the Erlenmeyer flask. The procedure is described below:

- In the first separating-funnel (tap turned off), 40 mmol of sodium metasilicate (11.368 g of nonahydrated product) and 120 mmol of sodium hydroxide were dissolved in 1 l of distilled and freshly decarbonated water,
- In the second separating-funnel (tap turned off), 100 mmol of calcium carbonate (10 g of solid $CaCO_3$) and 200 mmol of hydrochloric acid were dissolved in 1 l of distilled and decarbonated water. The reaction described in Eq. (A.3) occurred in the flask,

$$CaCO_3 + 2HCl \rightarrow CaCl_2 + H_2CO_3 \quad (A.3)$$

- Taps of the separating-funnels were then opened, and the two solutions were introduced simultaneously and mixed in the Erlenmeyer flask. Flows of the two solutions were identical, so that the stoichiometry of Reaction (A.2) was respected. Reaction products were then decanted in the Erlenmeyer flask for at least 12 h,
- A centrifugation was carried out several times, in order to separate the solid phase from the solution and extract the free ions,
- Finally, C-S-H pastes were vacuum dried at 20 °C, until weight stabilisation. A theoretical batch of 2.55 g was expected when using the specified quantities of reactive products. The material was then stored in a dessiccator.

The identity and the purity of the product were controlled by X-ray diffraction analysis: a main peak confirmed the presence of calcium silicate hydrate.

A.3. Preparation of ettringite

The process consisted of mixing saturated lime water with an aluminium sulphate solution, with respect to the stoichiometry of Reaction (A.4).

$$Al_2(SO_4)_3{\cdot}18H_2O + 6Ca(OH)_2 + 8H_2O \rightarrow 3CaO{\cdot}Al_2O_3{\cdot}3CaSO_4{\cdot}32H_2O \quad (A.4)$$

Centrifuging was then carried out, and the precipitate was vacuum dried at 25 °C for 7 days.

References

[1] P.C. Aïtcin, The durability characteristics of high performance concrete: a review, Cem. Concr. Compos. 25 (2003) 409–420.
[2] F.M. Fowkes, M.A. Mostafa, Acid–base interactions in polymer adsorption, Ind. Eng. Chem. Prod. Res. Dev. 17 (1978) 3–7.
[3] F.M. Fowkes, Attractive forces at interfaces, Ind. Eng. Chem. 56 (1964) 40–45.
[4] R.S. Farinato, S.S. Kaminski, J.L. Courter, in: K.L. Mittal (Ed.), Acid–base Interactions: Relevance to Adhesion and Technology, Utrech VSP, 1991, p. 171.
[5] F.M. Fowkes, D.O. Tischler, J.A. Wolfe, L.A. Lannigan, C.M. Ademu-John, M.J. Halliwell, Acid–base complexes of polymers, J. Polym. Sci., Polym. Chem. Ed. 22 (1984) 547–566.
[6] J.C. van Oss, R.J. Good, M.K. Chaudhury, Additive and nonadditive surface tension components and the interpretation of contact angles, Langmuir 4 (1988) 884–891.
[7] T.K. Kwei, E.M. Pearce, F. Ran, J.P. Chen, Hydrogen bonding in polymer mixtures, J. Appl. Polym. Sci., Polym. Phys. 24 (1986) 1597–1609.
[8] F.L. Riddle Jr., F.M. Fowkes, Spectral shifts in acid–base chemistry: Part 1. Van der Waals contributions to acceptor numbers, J. Am. Chem. Soc. 112 (1990) 3259–3264.
[9] M.M. Chehimi, J.F. Watts, S.N. Jenkins, J.E. Castle, X-ray photoelectron spectroscopy investigations of acid–base interactions in adhesion, J. Mater. Chem. 2 (1992) 209–215.
[10] F.M. Fowkes, Quantitative characterisation of the acid–base properties of solvents, polymers and inorganic surfaces, J. Adhes. Sci. Technol. 4 (1990) 669–691.
[11] D.R. Lloyd, T.C. Ward, H. Schreiber (Eds.), Inverse Gas Chromatography, Characterization of Polymers and Other Materials, ACS Symp. Series, vol. 391, American Chemical Society, Washington, DC, 1989.
[12] P. Mukhopadhyay, H.P. Schreiber, Aspects of acid–base interactions and the use of inverse gas chromatography: a review, Colloids Surf., A Physicochem. Eng. Asp. 100 (1995) 47–71.
[13] U. Panzer, H. Schreiber, On the evaluation of surface interactions by inverse gas chromatography, Macromolecules 25 (1992) 3633–3637.
[14] M.N. Belgacem, A. Gandini, Inverse gas chromatography as a tool to characterise dispersive and acid–base properties of the surface of fibers and powders, Surfactant Sci. Ser. 80 (1999) 41–124.
[15] Z.Y. Al-Saigh, Recent advances in the characterisation of polymers and polymers blends using the inverse gas chromatography method, Polym. News 19 (1994) 269–279.
[16] M.M. Chehimi, M.-L. Abel, C. Perruchot, M. Delamar, S.F. Lascelles, S.P. Armes, The determination of the surface energy of conducting polymers by inverse gas chromatography at infinite dilution: a review, Synth. Met. 104 (1999) 51–59.
[17] T. Hamieh, M. Nardin, M. Rageul-Lescouët, H. Haïdara, J. Schultz, Study of acid–base interactions between some metallic oxides and model organic molecules, Colloids Surf., A Physicochem. Eng. Asp. 125 (1997) 155–161.
[18] G. Ligner, A. Vidal, H. Balard, E. Papirer, London component of the surface energy of heat-treated silicas, J. Colloid Interface Sci. 133 (1989) 200–210.
[19] E. Papirer, J.-M. Perrin, B. Siffert, G. Philipponneau, Surface characteristics of aluminas in relation with polymer adsorption, J. Colloid Interface Sci. 144 (1991) 263–270.
[20] C.S. Flour, E. Papirer, Gas–solid chromatography: a method of measuring surface free energy characteristics of short glass fibers: Part 2. Through retention volumes measured near zero surface coverage, Ind. Eng. Chem. Prod. Res. Dev. 21 (1982) 666–669.
[21] F.M. Fowkes, D.W. Dwight, D.A. Cole, T.C. Huang, Acid–base properties of glass surfaces, J. Non-Cryst. Solids 120 (1990) 47–60.
[22] B. Riedl, H. Chtourou, Interactions in cellulose–polyethylene papers as obtained through inverse gas chromatography, Surfactant. Sci. Ser. 80 (1999) 125–143.
[23] A. Vukov, D.G. Gray, Adsorption of *n*-alkanes on carbon fibers at zero surface coverage, Langmuir 4 (1988) 743–748.
[24] E. Papirer, H. Balard, Inverse gas chromatography: a method for the evaluation of the interaction potential of solid surfaces, Surfactant. Sci. Ser. 80 (1999) 145–171.
[25] T.J. Bandosz, J. Jagiello, B. Andersen, J.A. Schwarz, Inverse gas chromatography study of modified smectite surfaces, Clays Clay Miner. 40 (1992) 306–310.
[26] A. Saada, E. Papirer, H. Balard, B. Siffert, Determination of the surface properties of illites and kaolinites by inverse gas chromatography, J. Colloid Interface Sci. 175 (1995) 212–218.
[27] E. Morales, M.V. Dabrio, C.R. Herrero, J.L. Acosta, Acid–base characterisation of sepiolite by inverse gas chromatography, Chromatographia 31 (1991) 357–361.
[28] H. Balard, A. Saada, J. Hartmann, O. Aoudj, E. Papirer, Estimation of the surface energetic heterogeneity of fillers by inverse gas chromatography, Makromol. Chem., Macromol. Symp. 108 (1996) 63–80.
[29] J. Jagiello, E. Papirer, A new method of evaluation of specific surface area of solids using inverse gas chromatography at infinite dilution, J. Colloid Interface Sci. 142 (1991) 232–235.
[30] T.J. Bandosz, K. Putyera, J. Jagiello, J.A. Schwarz, Application of inverse gas chromatography to the study of the surface properties of modified layered minerals, Microporous Mater. 1 (1993) 73–79.
[31] V. Oliva, B. Mrabet, M.I. Baeta Neves, M.M. Chehimi, K. Benzarti, Characterisation of cement pastes by inverse gas chromatography, J. Chromatogr., A 969 (2002) 261–272.
[32] M.I. Baeta Neves, V. Oliva, B. Mrabet, C. Connan, M.M. Chehimi, M. Delamar, S. Hutton, A. Roberts, K. Benzarti, Surface chemistry of cement pastes: a study by X-ray photoelectron spectroscopy, Surf. Interface Anal. 33 (2002) 834–841.
[33] L. Divet, Les reactions sulfatiques internes au béton: contribution à l'étude des mécanismes de la formation différée de l'ettringite, Etud. Rech. Labor. Ponts Chaussées ERLPC OA 40 (2001) 90–91.
[34] All details on XPS equipment available on Thermo VG Scientific web site: www.thermovgscientific.com.
[35] E.F. Meyer, On thermodynamics of adsorption using gas–solid chromatography, J. Chem. Educ. 57 (1980) 120–124.
[36] G.M. Dorris, D.G. Gray, Adsorption of *n*-alkanes at zero surface coverage on cellulose paper and wood fibers, J. Colloid Interface Sci. 77 (1980) 353–362.
[37] D.J. Brookman, D.T. Sawyer, Specific interactions affecting gas chromatographic retention for modified alumina columns, Anal. Chem. 40 (1968) 106–110.
[38] C. Saint Flour, E. Papirer, Gas–solid chromatography: a quick method of estimating surface free energy variations induced by treatment of short glass fibers, J. Colloid Interface Sci. 91 (1983) 69–75.

[39] P. Koning, T.C. Ward, R.D. Allen, J.E. McGrath, Thermodynamics of acid–base polymer/solute interactions via inverse gas chromatography, ACS Polym. Prep. 26 (1985) 189–190.
[40] J. Schultz, L. Lavielle, in: D.R. Lloyd, T.C. Ward, H.P. Schreiber (Eds.), Inverse Gas Chromatography. Characterisation of Polymers and Others Materials, ACS Symp. Series, vol. 391, American Chemical Society, Washington, DC, 1989, Ch. 14.
[41] E. Osmont, H.P. Schreiber, in: D.R. Lloyd, T.C. Ward, H.P. Schreiber (Eds.), Inverse Gas Chromatography. Characterisation of Polymers and Others Materials, ACS Symp. Series, vol. 391, American Chemical Society, Washington, DC, 1989, Ch. 17.
[42] J.B. Donnet, S.J. Park, H. Balard, Evaluation of specific interactions of solid surfaces by inverse gas chromatography, Chromatographia 31 (1991) 434–440.
[43] A.C Tiburcio, J.A Manson, Acid–base interactions in filler characterisation by inverse gas chromatography, J. Appl. Polym. Sci. 42 (1991) 427–438.
[44] M.M. Chehimi, E. Pigois-Landureau, Determination of acid–base properties of solid materials by inverse gas chromatography at infinite dilution, J. Mater. Chem. 4 (1994) 741–745.
[45] M.N. Belgacem, A. Gandini, in: E. Pefferkorn (Ed.), Interfacial Phenomena in Chromatography, vol. 80, Marcel Dekker Inc., New York, 1999, p. 41.
[46] L. Black, K. Garbev, P. Stemmermann, K.R. Hallam, G.C. Allen, Characterisation of crystalline C-S-H phase by X-ray photoelectron spectroscopy (XPS), Cem. Concr. Res. 33 (6) (2003) 899–911.
[47] L. Black, K. Garbev, A. Stumm, K. Garbev, P. Stemmermann, K.R. Hallam, G.C. Allen, Photoelectron analysis of cement clinker phases, Cem. Concr. Res. 33 (10) (2003) 1561–1565.
[48] S. Long, C. Liu, Y. Wu, ESCA study on the early C_3S hydration in NaOH solution and pure water, Cem. Concr. Res. 28 (2) (1998) 245–249.
[49] D.S. Keller, P. Luner, Surface energetics of calcium carbonates using inverse gas chromatography, Colloids Surf., A Physicochem. Eng. Asp. 161 (2000) 401–415.
[50] H.P. Schreiber, F. Saint Germain, Specific interactions and their effect on the properties of filled polymers, J. Adhes. Sci. Technol. 4 (1990) 319–331.
[51] E. Brendlé, E. Papirer, A new topological index for molecular probes used in inverse gas chromatography for the surface nanorugosity evaluation, J. Colloid Interface Sci. 194 (1997) 207–216.
[52] G. Ligner, M. Sidqi, J. Jagiello, H. Balard, E. Papirer, Characterisation of specific interactions capacity of solid surfaces by adsorption of alkanes and alkenes. Adsorption on crystalline silica layer surfaces. Part 2, Chromatographia 29 (1990) 35–38.
[53] C.J. van Oss, M.K. Chaudhury, R.J. Good, Interfacial Lifshitz-van der Waals and polar interactions in macroscopic systems, Chem. Rev. 88 (1988) 927–941.
[54] P.E. Vickers, J.F. Watts, C. Perruchot, M.M. Chehimi, The surface chemistry and acid–base properties of PAN-based carbon fibre, Carbon 38 (2000) 675–689.